Acta Biochim Biophys Sin, 2015, 47(3), 199–206
doi: 10.1093/abbs/gmv002
Advance Access Publication Date: 7 February 2015
Original Article

Original Article

Biochemical and structural characterization of MUPP1-PDZ4 domain from *Mus musculus*

Haili Zhu[1], Zexu Liu[2], Yuxin Huang[1], Chao Zhang[1], Gang Li[3], and Wei Liu[1,2,*]

[1]Shenzhen Key Laboratory for Neuronal Structural Biology, Biomedical Research Institute, Shenzhen Peking University-The Hong Kong University of Science and Technology Medical Center, Shenzhen 518036, China, [2]Division of Life Science, State Key Laboratory of Molecular Neuroscience, Hong Kong University of Science and Technology, Hong Kong, China, and [3]Department of Biochemistry and Molecular Biology, School of Basic Medical Sciences, Peking University Health Science Center, Beijing 100191, China

*Correspondence address. Tel/Fax: +86-755-83910721; E-mail: liuw@ust.hk

Received 12 October 2014; Accepted 10 December 2014

Abstract

Specific protein–protein interactions are important for biological signal transduction. The postsynaptic density-95, disc-large, and zonulin-1 (PDZ) domain is one of the most abundant protein interaction modules. Multi-PDZ-domain protein 1 (MUPP1), as a scaffold protein, contains 13 PDZ domains and plays an important role in cytoskeletal organization, cell polarity, and cell proliferation. The study on PDZ domain of MUPP1 helps to understand the mechanisms and functions of MUPP1. In the present study, the fourth PDZ domain of MUPP1 (MUPP1-PDZ4) from *Mus musculus* was cloned, expressed, purified, and characterized. The MUPP1-PDZ4 domain was subcloned into a pET-vector and expressed in *Escherichia coli*. Affinity chromatography and size-exclusion chromatography were used to purify the protein. MUPP1-PDZ4 protein was a monomer with a molar mass of 16.4 kDa in solution and had a melting point of 60.3°C. Using the sitting-drop vapor-diffusion method, MUPP1-PDZ4 protein crystals were obtained in a solution (pH 7.0) containing 2% (v/v) polyethylene glycol 400, 0.1 M imidazole, and 24% (w/v) polyethylene glycol monoethyl ether 5000. Finally, the crystal was diffracted with 1.6 Å resolution. The crystal structure showed that MUPP1-PDZ4 domain contained three α-helices and six β-strands in the core. The GLGI motif, L562/A564 on the β-strand B, and H605/V608/L612 on the α-helix B formed a PDZ binding pocket which could bind to the C-terminal of the binding partners. This biochemical and structural information will provide insights into how PDZ binds to its target peptide and the theoretical foundation for the function of MUPP1.

Key words: MUPP1, PDZ domain, crystallization

Introduction

Biological signal transduction from receptors at the plasma membrane to their targets in the cytoplasm and nucleus relies on specific protein–protein interactions [1]. Through protein–protein interactions, diverse biological activities are regulated [2]. Thus, it is very important to elucidate the mechanisms involved in these protein–protein interactions.

Since protein–protein interactions mainly depend on their domain–domain interactions [3], how protein domains interact with each other is critical for protein interactions and their functions. The postsynaptic density-95, disc-large, and zonulin-1 (PDZ) domain has become one of the most abundant protein interaction modules in various species. There are 90,165 PDZ domains in 58,998 proteins included in the SMART's (http://smart.embl-heidelberg.de/) NRDB database (non-redundant database) [4]. Because a number of biology dysfunctions are related to PDZ-mediated interactions [5–8], there is a growing interest in studying the interaction between PDZ domains and their binding partners which may become drug targets.

A typical PDZ domain contains ~90 amino acid residues which form six β-strands and two α-helices. Most commonly, PDZ domains recognize the extreme C-terminal of target proteins. In some cases, PDZ domains can also recognize the internal sequence of target proteins [9,10]. PDZ domains are mostly found in submembrane scaffolding proteins which often contain multiple copies of PDZ domains and play important roles in organizing signaling cascades. Multi-PDZ-domain protein 1 (MUPP1) is one of the scaffold proteins containing 13 PDZ domains and has no apparent catalytic motifs. Through the PDZ-domain-mediated interaction with the target proteins, MUPP1 acts as a platform to make the signaling proteins associated with each other and to form large molecular weight signaling complexes, which largely improves the efficiency, specificity, and sensitivity of the chemical reaction within the complexes compared with freely diffused reactants [1,11].

MUPP1 was first discovered to bind to the C-terminal of 5-HT2C receptor in the yeast two-hybrid experiments. It was named as MUPP1 for containing multiple PDZ domains (from 10 to 13 in different species) [12]. The *MUPP1* gene is localized on human chromosome 9p24-p22 and includes 19 transcripts due to alternative splicing and 11 encoding-transcripts. Among the transcripts, the longest transcript encodes ~2000 amino acid-long MUPP1 which is abundant in the brain as well as in several peripheral organs [13]. MUPP1 regulates cell processes such as cytoskeletal organization, cell polarity, cell proliferation, and many signal transduction pathways through its PDZ domains [14,15]. The *MUPP1* gene is associated with some human diseases [16,17] and its mutations have been found in human congenital hydrocephalus [18], leber congenital amaurosis, and retinitis pigmentosa [19]. *MUPP1*'s roles in ethanol withdrawal and voluntary ethanol consumption have already been confirmed in MUPP1 transgenic and knockdown mouse models [20].

Until now, the structures for the 1st (PDB code: 2O2T), 3rd (PDB code: 2IWN), 7th (PDB code: 2IWQ and 2FCF), 10th (PDB code: 2POPG), 11th (PDB code: 2QG1), 12th (PDB code: 2IWP and 2IWO), and 13th (PDB code: 2FNE) PDZ domains of MUPP1 have been resolved [5], and some binding partners have been identified such as CLAUDIN1 [21], CLAUDIN8 [22], JAM1 [21], RhoGEF-Tech [14], Mt1 melatonin receptor [23], and NG2 [24]. Great progress has been made in the study of functional properties of MUPP1; however, the underlying molecular mechanisms are still poorly understood. Therefore, a better characterization of PDZ domains in MUPP1 may become essential in understanding the function of MUPP1. In this study, MUPP1-PDZ4 protein was expressed, purified, and characterized biochemically and structurally.

Materials and Methods

Materials

Enzymes were obtained from New England Biolabs (Ipswich, USA). DTT, NaCl, Tris, and ethylenediaminetetraacetic acid (EDTA) were obtained from Sigma (St Louis, USA). Other chemicals of analytical reagent grade were purchased from Sangon (Shanghai, China).

Plasmids

The cDNAs encoding MUPP1-PDZ4 (residues 521–630 and 521–665) from *Mus musculus* were amplified by polymerase chain reaction (PCR) from a mouse brain cDNA library. MUPP1-PDZ4$_{521–630}$ and $_{521–665}$ cDNA sequences were amplified using forward primer (CGGATCCGCTGAAGATGTGCAGCAAGAG) and reverse primers (GGAATTCTCAGGGTGGCACAGTCCGACGGCAG/GGAATTCTCAATCCTCTGTCTCTGAGGACCCA), which introduced 5′ *Bam*HI and 3′ *Eco*RI restriction sites for parallel cloning. The PCR-amplified MUPP1-PDZ4$_{521–630}$ and MUPP1-PDZ4 $_{521–665}$ were subcloned into a modified version of the pET32a vector [11]. The cDNA encoding 5HT2C peptide (SVVSERISSV) and Syx peptide (LNSTLTASEV) were subcloned into pETMG.3C vector (a vector contains a six His-tagged GB1 fusion carrier protein) by primer-annealing methods [25]. The primers for 5HT2C peptide and Syx peptide were synthesized as the following sequences, respectively: GATCCAATGTGGTCAGCGAGAGGATTAGTAGTGTGTAAG/AATTCTTACACACTACTAATCCTCTCGCTGACCACATTG and GATCCCTCAACTCCACGCTCACTGCCTCGGAGGTGTGAG/GATCCTCACACCTCCGAGGCAGTGAGCGTGGAGTTGAGG.

Protein expression and purification

The pET-MUPP1-PDZ4 plasmids were transformed into *Escherichia coli* BL21 (DE3) strain. Then single colony was inoculated to Luria–Bertani (LB) media containing 50 μg/ml ampicillin and induced by 0.1 mM isopropyl β-D-1-thiogalactopyranoside at 16°C for 20 h. The cells were harvested by centrifugation at 6000 *g* for 10 min, lysed by sonication for 20 min and finally centrifuged at 20,000 *g* for 20 min to collect the supernatant. Then, the supernatants were purified by Ni^{2+}-Sepharose (GE Healthcare, Little Chalfont, UK) affinity chromatography, followed by a size-exclusion chromatography (Hiload 26/60 Superdex 200; GE Healthcare) in a buffer of 50 mM Tris, pH 7.5, containing 100 mM NaCl, 1 mM DTT, and 1 mM EDTA [11]. The N-terminal His-tagged fragments were then cleaved by 3C protease at 25°C overnight and the cleavage was monitored by sodium dodecyl sulfate–polyacrylamide gel electrophoresis (SDS–PAGE). After being totally cleaved, the protein was purified by another step of size-exclusion chromatography. The purified proteins were analyzed by 15% SDS–PAGE. Finally, the absorptions at 280 nm were measured and protein concentrations were determined by Lambert–Beer law. The extinction coefficients for MUPP1-PDZ4 were determined using the online software 'ProtParam' from the Bioinformatics Resource Portal [26]. The two GB1-tagged peptides were also purified by Ni^{2+}-Sepharose affinity chromatography, followed by a size-exclusion chromatography. To check the purity of MUPP1-PDZ4, SDS–PAGE was performed using a 5% stacking gel and a 15% separating gel in Tris–glycine buffer. The purified protein (6 μg) was loaded into each lane. The PageRuler Prestained Ladder was used as the protein mass standard (Fermentas, Waltham, USA). Electrophoresis was run in a vertical electrophoresis Mini-PROTEAN Tetra Cell Apparatus (Bio-Rad, Hercules, USA). Gels were stained with Coomassie Blue R250 [27].

Size-exclusion chromatography and multi-angle laser light scattering

Size-exclusion chromatography was performed on a Superose 12 10/300 GL column (GE Healthcare), pre-equilibrated with 50 mM Tris, pH 7.5, containing 100 mM NaCl, 1 mM DTT, and 1 mM EDTA. The AKTA chromatography system (GE Healthcare) was coupled to a Dawn Heleos-II light scattering detector (Wyatt Technologies, Clinton, USA) and an Optilab-Rex refractive index monitor (Wyatt Technologies). The purified protein (80 μg) was loaded and the column was eluted with 50 mM Tris, pH 7.5, containing 100 mM NaCl, 1 mM DTT, and 1 mM EDTA at a flow rate of 0.8 ml/min. Molecular mass was calculated by using ASTRA software (Wyatt Technologies) [28]. The system was calibrated with bovine serum albumin whose theoretical molar mass is 66.4 kDa.

Circular dichroism measurement

Circular dichroism (CD) spectra were obtained by using Applied Photophysics Chirascan instrument (Applied Photophysics, Surrey, UK) with a thermostated cell holder. A quartz cell with a 0.5-mm light path was used. Spectra were recorded from 200 to 260 nm for the far-ultraviolet (UV) CD. The final concentration of MUPP1-PDZ4 was kept at 30 μM. The spectra were corrected relative to the buffer blank. Temperature-dependent denaturation measurements were performed at temperatures from 25.0 to 93.0°C [29]. The unfolding of MUPP1-PDZ4 domain was assumed to undergo a two-state transition, $N \Leftrightarrow U$, where N and U represent the native state and unfolded state, respectively. The equilibrium constant for this unimolecular reaction is determined by the following equation:

$$K = \frac{U}{N} = \frac{f}{1-f}, \quad (1)$$

where f is the fraction of unfolded protein which can be obtained from the CD signal change during the thermal denaturation.

Through equation (1) and the Van't Hoff equation: $\mathrm{d} \ln K/\mathrm{d}T = \triangle H/RT^2$ [30,31], the T_m value and the Van't Hoff enthalpy can be obtained.

Crystallography

Freshly purified MUPP1-PDZ4 was concentrated to 0.5 mM. Crystals of MUPP1-PDZ4 were obtained at 16°C by sitting-drop vapor diffusion against 80 μl well solution using 96-well format crystallization plates. One crystal form was obtained. Crystals belonging to space group $I222$ were obtained with a well solution (pH 7.0) containing 2% (v/v) polyethylene glycol 400, 0.1 M imidazole, and 24% (w/v) polyethylene glycol monoethyl ether 5000. Crystals were flash-cooled in liquid nitrogen. A 1.65 Å resolution X-ray data-set was collected at Shanghai Synchrotron Radiation Facility (Shanghai, China) and processed using HKL2000 [32]. The initial phase was determined by molecular replacement using SAP102-PDZ3 (PDB code: 3JXT) as a searching model. The model was refined in Refmac5 [33] and Phenix [34] against the 1.65 Å data-set. Further model building and adjustments were completed using COOT [35]. The refinement statistics is listed in Table 1. All structure figures were prepared by PyMOL (www.pymol.org). The sequence alignments were prepared and presented using ClustalW [36] and ESPript [37], respectively.

Table 1. Statistics of data collection and model refinement

Data collection	
Space group	*I*222
Unit cell parameters (Å)	$a = 51.1$, $b = 52.7$, $c = 96.8$
Resolution range (Å)	50.00–1.65 (1.68–1.65)
Number of unique reflections	16,041 (789)
Redundancy	7.2 (7.8)
I/σ	48.2 (3.7)
Completeness (%)	99.4 (100)
R_{merge} (%)[a]	7.2 (77.3)
Structure refinement	
Resolution range (Å)	50.00–1.65 (1.75–1.65)
R_{cryst}/R_{free} (%)[b]	17.3(20.8)/20.4 (29.7)
RMSD bonds (Å)/angle(°)	0.012/1.37
Average *B* factor	28.68
Number of atoms	
Protein atoms	810
Water molecules	99
Ligands	5
Number of reflections	
Working set	15,226
Test set	805
Ramachandran plot[c]	
Favored regions (%)	100
Allowed regions (%)	0
Outliner (%)	0

Numbers in parentheses represent the value for the highest resolution shell.

[a] $R_{merge} = \sum|I_i - I_m|/\sum I_i$, where I_i is the intensity of the measured reflection and I_m is the mean intensity of all symmetry-related reflections.

[b] $R_{cryst} = \Sigma||F_{obs}| - |F_{calc}||/\Sigma|F_{obs}|$, where F_{obs} and F_{calc} are observed and calculated structure factors. $R_{free} = \Sigma T||F_{obs}| - |F_{calc}||/\Sigma T|F_{obs}|$, where T is a test data-set of ~5% of the total reflections randomly chosen and set aside prior to refinement.

[c] Defined by MolProbity.

Analytical gel-filtration chromatography

Analytical gel-filtration chromatography was performed on an AKTA FPLC system using a Superose 12 10/300 GL column. Protein samples were loaded onto the column equilibrated with 50 mM Tris–HCl buffer (pH 7.5), containing 100 mM NaCl, 1 mM DTT, and 1 mM EDTA. About 50 μM MUPP1-PDZ4 was mixed with 50 μM

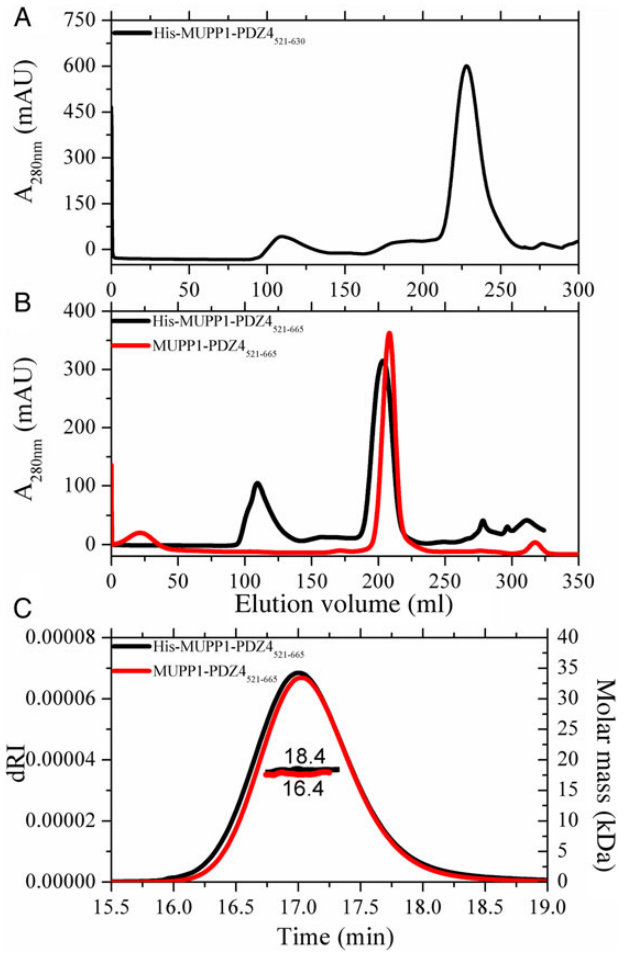

Figure 1. Purification of MUPP1-PDZ4 and determination the molecular mass of MUPP1-PDZ4 The purification of MUPP1-PDZ4$_{521-630}$ (A) and $_{521-665}$ (B) using gel-filtration chromatography on Hiload 26/60 Superdex 200 column. (C) The molecular mass of MUPP1-PDZ4 was measured by the SEC-MALS method. About 80 μg sample was loaded into the size-exclusion column in each experiment. The black line represented the protein His-MUPP1-PDZ4 and the red line represented the protein MUPP1-PDZ4.

GB1-tagged 5HT2C peptide (SVVSERISSV) or GB1-tagged Syx peptide (LNSTLTASEV). The mixtures had been incubated for 15 min at 25°C, centrifuged at 14,000 *g* for 15 min and loaded to the injector. The column was eluted at a flow rate of 0.8 ml/min. When the proteins were mixed and injected to the gel-filtration column, the association of the proteins will result in the formation of a larger protein complex and the decrease of their elution volume in the column.

Isothermal titration calorimetry measurement

Isothermal titration calorimetry (ITC) measurements were carried out on a MicroCal iTC200 calorimeter (GE Healthcare) to measure the binding affinities between peptides and MUPP1-PDZ4. All samples were prepared in 50 mM Tris–HCl buffer (pH 7.5), containing 100 mM NaCl, 1 mM DTT, and 1 mM EDTA. All experiments were performed at 25°C. The MUPP1-PDZ4 was loaded into the sample cell and the peptides were placed in the injection syringe. The sample in the injection syringe was sequentially titrated into the sample cell (0.5 μl for the first injection and 2 μl each for the following 19 injections in this study).The enthalpy change (ΔH) of each injection was recorded by the calorimeter, which created a curved thermogram (a plot of enthalpy change vs. injection volume). Combined with two thermodynamic equations ($\Delta G = -nRT \ln K_a$ and $\Delta G = \Delta H - T\Delta S$), several thermodynamic parameters of this interaction can be obtained by fitting this curve using a single set of identical sites model. These parameters include: the standard molar enthalpy change (ΔH), the standard entropy change (ΔS), the association constant (K_a), and the binding stoichiometry (n) [38].

Results

Purification of recombinant proteins

Mus-MUPP1 was a 2055-residue multiple PDZs protein (13 PDZ domains). The boundary of MUPP1-PDZ4 was determined to be residues 521–630 according to the secondary structure prediction by the website of psipred (http://bioinf.cs.ucl.ac.uk/psipred/). The plasmid for this boundary was first constructed and the protein His-MUPP1-PDZ4$_{521–630}$ was expressed and purified. Unfortunately, there were two bands on the gel which indicated that the His-MUPP1-PDZ4$_{521–630}$ protein was not suitable for further experimental characterization (**Figs. 1A** and **2A**). Then, another boundary containing residues 521–665 with an extra C-terminal sequence of 35 amino acids was constructed and the protein was expressed and purified. **Figures 1B** and **2B** showed the purity of recombinant His-MUPP1-PDZ4$_{521–665}$, which was only one band. After the two-step purification, His-tag fragment at the N-terminal was cleaved. MUPP1-PDZ4$_{521–665}$ without the N-terminal His-tag also showed a single band on the SDS–PAGE gel and the sequence was GPGSAEDVQQEAALLTKWQRIMGINYEIV VAHVSKFSENSGLGISLEATVGHHFIRSVLPEGPVGHSGKLFSGD ELLEVNGINLLGENHQDVVNILKELPIDVTMVCCRRTVPPIALS EMDSLDINDLELTEKPHIDLGEFIGSSETED.

The absolute molar mass of the MUPP1-PDZ4$_{521–665}$ with and without His-tag was determined by size-exclusion chromatography and multi-angle laser light scattering (SEC-MALS). As shown in **Fig. 1C**, there was one sharp and symmetrical peak showing that the protein MUPP1-PDZ4 was pure. The theoretical molar mass of the MUPP1-PDZ4$_{521–665}$ was 16.2 kDa and the molar mass of

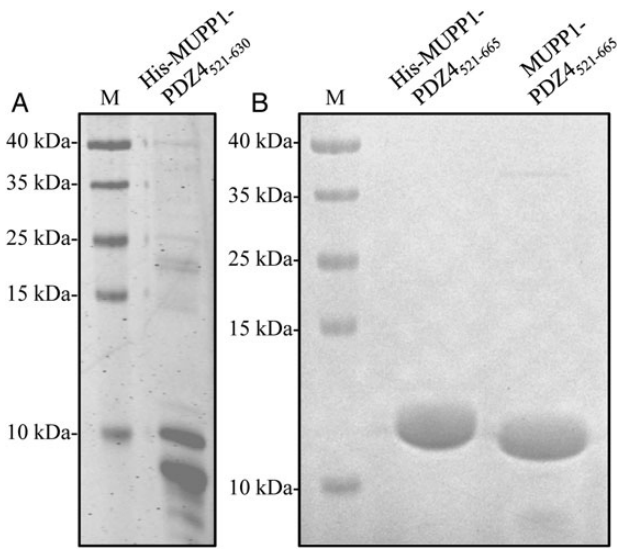

Figure 2. SDS–PAGE of the protein MUPP1-PDZ4$_{521–630}$ and $_{521–665}$ About 6 μg protein per lane was loaded into the gel and the gels were visualized by Coomassie Blue R250 staining. (A) SDS–PAGE result of His-MUPP1-PDZ4$_{521–630}$. Lane M is the protein marker. The purity for His-MUPP1-PDZ4$_{521–630}$ was ~60% and not suitable for further study. (B) SDS–PAGE of His-MUPP1-PDZ4$_{521–665}$ and MUPP1-PDZ4$_{521–665}$. Lane M is the protein marker. The purity of MUPP1-PDZ4$_{521–665}$ was >95%.

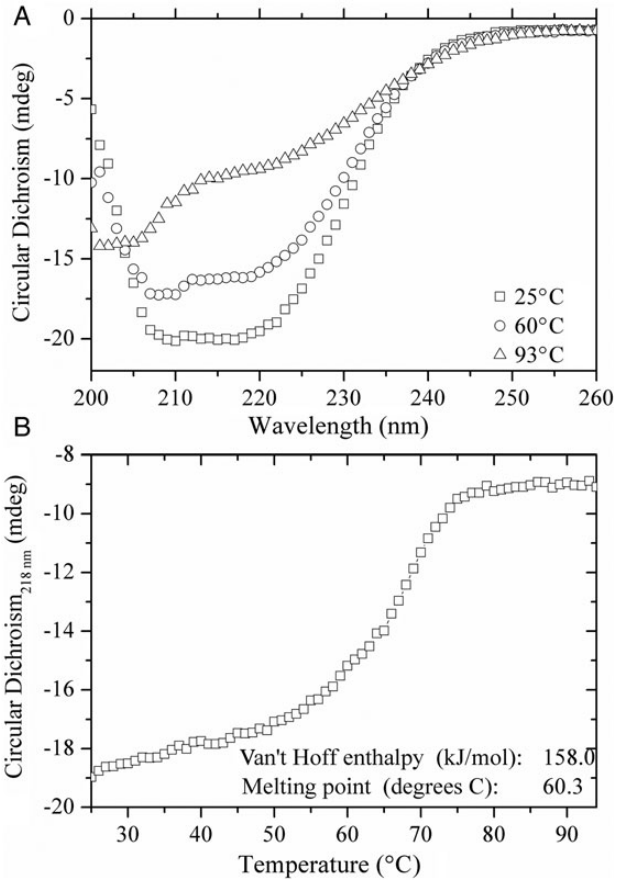

Figure 3. The thermal stability of MUPP1-PDZ4 monitored by CD spectroscopy (A) Far-UV CD spectra of MUPP1-PDZ4 at 25°C (open square), 60°C (open circle), and 93°C (open up triangle) represented three status of the protein which were folded, half-folded, and unfolded, respectively. (B) Effect of temperature on the relative change in the β-sheet content of MUPP1-PDZ4 protein, determined by monitoring the CD signal at 218 nm.

N-terminal His-tagged MUPP1-PDZ4$_{521–665}$ was 18.2 kDa, while the experimentally measured molar mass from MALS were 16.4 and 18.4 kDa, respectively (0.5% fitting error) (**Fig. 1C**). According to the analysis of SEC-MALS results, it was concluded that MUPP1-PDZ4$_{521–665}$ was a monomer with 16.4 kDa molar mass in solution.

Stability of MUPP1-PDZ4

CD spectroscopy was used to detect the secondary structure of MUPP1-PDZ4. As shown in **Fig. 3A**, the CD spectrum for MUPP1-PDZ4 had typical negative peaks around 210 and 220 nm, indicating α-helix and β-stand structure, while the CD signal at 200 nm reflects the random coil structure. The value of $CD_{218\ nm}$ of MUPP1-PDZ4 increased gradually from –20 to –9 mdeg when the incubation temperature was gradually increased from 25.0 to 93.0°C. The curves at 25, 60, and 93°C represent folded, half-folded, and unfolded status of MUPP1-PDZ4 domain, respectively. **Figure 3B** shows the plot of CD signal at 218 nm against different temperatures. The MUPP1-PDZ4 protein had a melting point of 60.3°C and the Van't Hoff enthalpy was 158 kJ/mol.

The CD data revealed that folded status MUPP1-PDZ4 contained α-helices and β-stands, with a melting point of 60.3°C. Thus, MUPP1-PDZ4 was stable in physical condition.

Crystal structure of MUPP1-PDZ4

We crystallized the MUPP1-PDZ4 domain and solved its structure at 1.6 Å resolution. Data collection and refinement statistics are shown in Table 1. A model for amino acid 521–629 had been built. Region from residues 630–665 was absent in the model because of its flexibility. All of the secondary structure elements and connecting loops were well ordered.

Sequence alignment analysis revealed that the MUPP1-PDZ4 domain was highly conserved during evolution (**Fig. 4A**). MUPP1-PDZ4 consists of a core of six β-strands (βA–βF) and three α-helices (α-extension, αA, and αB) as shown in **Fig. 4B**. The domain was

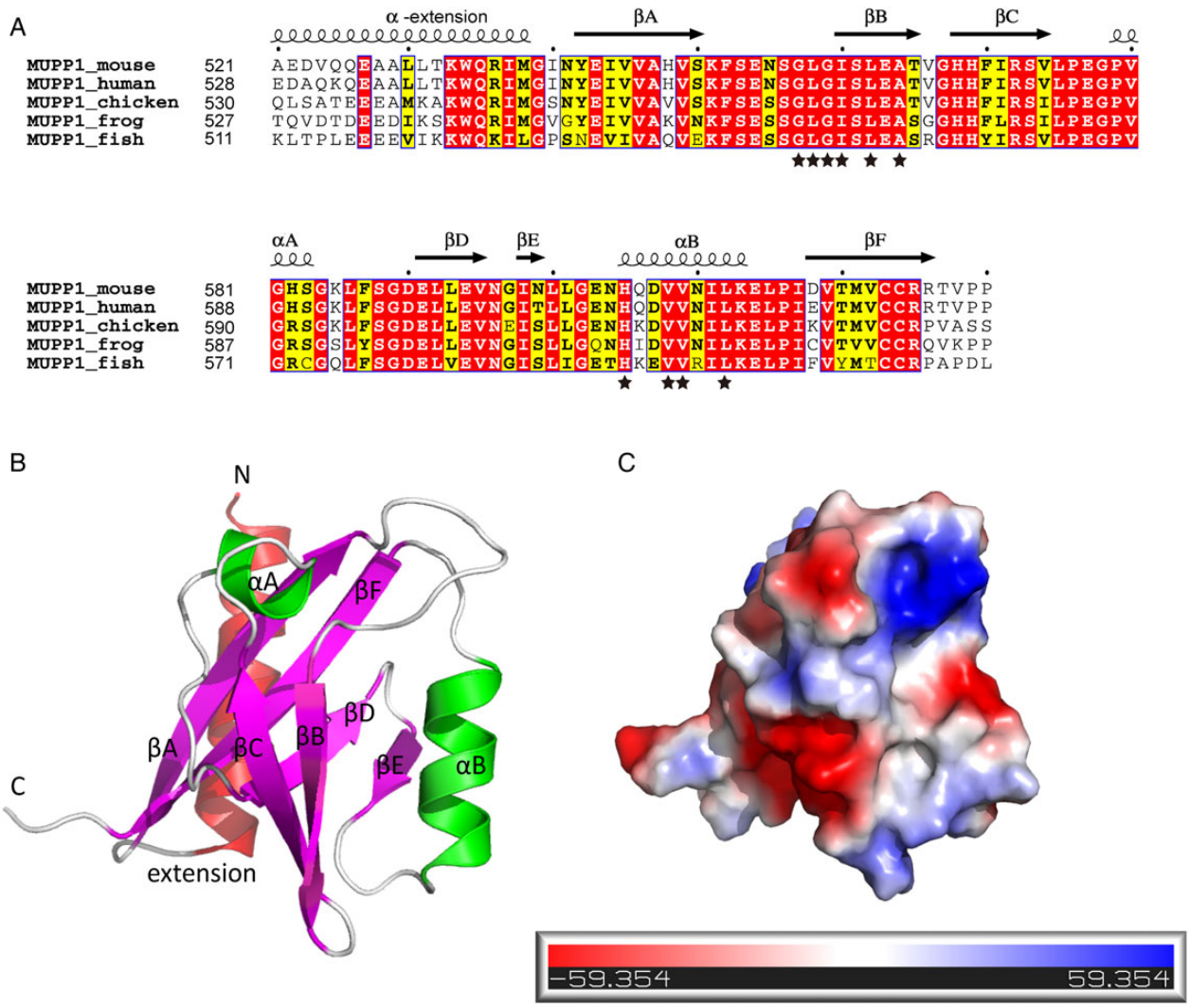

Figure 4. Sequence alignment and crystal structure of MUPP1-PDZ4 (A) Amino acid sequence alignment of the PDZ4 domains of the MUPP1 from different species. In this alignment, the absolutely conserved and highly conserved residues were highlighted in red and yellow, respectively. The secondary structure of PDZ4 determined from the crystal structure was indicated at the top of the sequence. The residues for the binding pocket were indicated with stars. (B) Ribbon diagram of the MUPP1-PDZ4 domain with secondary structure elements. (C) The vacuum electrostatics surface of the MUPP1-PDZ4 domain. Positively charged residues were shown as blue, negatively charged residues as red, and hydrophobic residues as white.

compact and globular (**Fig. 4C**). β-Strands formed a partially opened β-barrel, and the open sides of the barrel were each capped with an α-helix (αA and αB). Compared with the canonical PDZ domain, the structure of MUPP1-PDZ4 had an α-extension. But the function of this α-extension was still unclear. The GLGI motif on the carboxylate binding loop, L562/A564 on the βB, and H605/V608/L612 on the αB jointly formed a binding pocket for the binding of the carboxyl tail of the ligands (**Fig. 5**). The backbone amide groups of GLGI motif, G557, L558, G559, and I560 could form hydrogen bonds with the carboxylate of the ligands. H605 of the αB was a polar residue and preferentially bound to serine or threonine at the –2 position of the ligands. Hence, we hypothesized that the MUPP1-PDZ4 domain could bind a peptide with S/T(–2)-*X*(–1)-Φ(0) at the C-terminal, where *X* represented any residues and Φ represented hydrophobic residues.

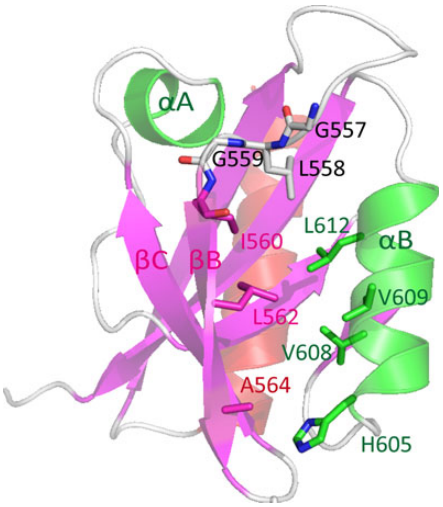

Figure 5. The combined stick model and the ribbon representation showing the hydrophobic binding pocket of MUPP1-PDZ4 Side chains forming the hydrophobic binding pocket were shown in atomic representation.

Binding property of MUPP1-PDZ4

In order to test our hypothesis for the binding property of MUPP1-PDZ4, two peptides [SVVSERISSV (5HT2C) and LNSTLTASEV (Syx)] containing S/T-*X*-Φ motif at the C-terminal were chosen, and the analytical gel filtration and ITC were used to detect the binding of two peptides with MUPP1-PDZ4. As shown in **Fig. 6**, these two peptides did not bind to MUPP1-PDZ4.

Discussion

Proteins containing PDZ domain play important roles in assembling protein complexes for signal transduction and organizing large,

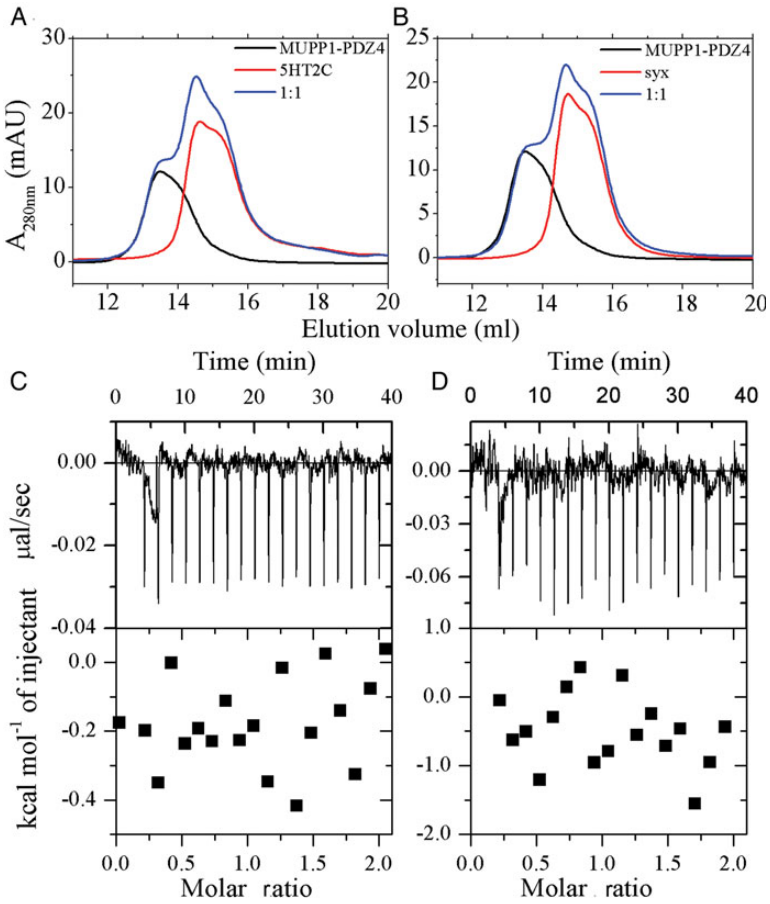

Figure 6. Analytical gel-filtration and ITC-based measurement for the binding of two peptides SVVSERISSV and LNSTLTASEV to MUPP1-PDZ4 (A,B) Analytical gel-filtration analysis between MUPP1-PDZ4 and two GB1-tagged peptides, showing that 1:1 MUPP1-PDZ4/GB1-tagged peptide mixture had no shift on their elution volume. (C,D) ITC-based measurement of MUPP1-PDZ4 titrating two GB1-tagged peptides, showing no interaction between MUPP1-PDZ4 and GB1-tagged peptides. The top panel presents typical calorimetric titration of two peptides with MUPP1-PDZ4 at 25°C. The bottom panel shows the plots of the heat (kcal) vs. the molar ratio of two peptides to MUPP1-PDZ4.

complicated cellular structures in neurons and epithelial cells [4]. The interactions between PDZ domains and their target proteins have been studied [2,7]. Some PDZ domains are targets for potential therapeutic applications in PDZ-domain-related human diseases [5,8].

MUPP1, as a scaffold protein, contains 13 PDZ domains. Various PDZ domains of MUPP1 can bind to diverse target proteins specifically, which is the base of the macromolecular assemblies [15]. MUPP1-PDZ4, the fourth PDZ of the protein, is highly conserved in different species according to amino acid sequences analysis. However, little is known about its function. In this study, the MUPP1-PDZ4 domain was purified and its biochemical characterization was performed. As shown in **Figs.** 4 and 5, the structure of MUPP1-PDZ4 was obtained through X-ray crystallography. It showed some differences when compared with the canonical PDZ domain. There was an α-extension beyond the PDZ domain, but its function was unclear. The C-terminal sequences binding to PDZ domain had been classified into three classes: I, II, and III. The amino acid sequence of class I was (S/T)-*X*-Φ, class II was Φ-*X*-Φ, and class III was (D/E)-*X*-Φ, where X represents any residues and Φ represents hydrophobic residues [39,40]. With the analysis of the residues in the binding pocket, it was found that the C-terminal sequence of the ligands should be S/T(–2)-*X*(–1)-Φ(0) and belonged to class I. However, two GB1-tagged peptides [SVVSERISSV (5HT2C) and LNSTLTASEV (Syx)] containing S/T-*X*-Φ motif at the C-terminal showed no binding to MUPP1-PDZ4 (**Fig.** 6). This interesting phenomenon indicated that the C-terminal S/T-*X*-Φ motif may not be enough for the MUPP1-PDZ4 binding. A longer candidate peptide should be tested to confirm this result.

In this study, the protein quality of MUPP1-PDZ4$_{521–665}$ was much better than MUPP1-PDZ4$_{521–630}$, indicating that the residues 631–665 were indispensable for the stability of PDZ4 domain. However, the electron density from residues 630–665 was absent in the crystal structure. Therefore, how the residues 631–665 could stabilize PDZ4 domain was still unknown.

Through binding to target proteins, MUPP1 plays an important role in cell migration and signal transduction. The study on the structure will provide a theoretical base for the subsequent function study of MUPP1 protein.

Accession number

The atomic coordinates and structure factors of the MUPP1-PDZ4 have been deposited in the Protein Data Bank under the accession code of 4XH7.

Acknowledgment

We thank the BL17U1 beamline team of the Shanghai Synchrotron Radiation Facility for the X-ray beam time.

Funding

This work was supported by the grants from the Natural Science Foundation of Guangdong Province (No. S2012010008170), the National Basic Research Program of China (No. 81300922 and No. 2014CB910200), the National Natural Science Foundation of China (No. 81072710, No. 81370522 and No. 31400647) and the Basic Research Program of Shenzhen City (No. JC201104220331A).

References

1. Zhang M, Wang W. Organization of signaling complexes by PDZ-domain scaffold proteins. *Acc Chem Res* 2003, 36: 530–538.
2. Lee HJ, Zheng JJ. PDZ domains and their binding partners: structure, specificity, and modification. *Cell Commun Signal* 2010, 8: 8.
3. Deng M, Mehta S, Sun F, Chen T. Inferring domain–domain interactions from protein–protein interactions. *Genome Res* 2002, 12: 1540–1548.
4. Nakariyakul S, Liu ZP, Chen L. A sequence-based computational approach to predicting PDZ domain-peptide interactions. *Biochim Biophys Acta* 2014, 1844: 165–170.
5. Elkins JM, Papagrigoriou E, Berridge G, Yang X, Phillips C, Gileadi C, Savitsky P, *et al*. Structure of PICK1 and other PDZ domains obtained with the help of self-binding C-terminal extensions. *Protein Sci* 2007, 16: 683–694.
6. Wen W, Wang W, Zhang M. Targeting PDZ domain proteins for treating NMDA receptor-mediated excitotoxicity. *Curr Top Med Chem* 2006, 6: 711–721.
7. Wang NX, Lee HJ, Zheng JJ. Therapeutic use of PDZ protein–protein interaction antagonism. *Drug News Perspect* 2008, 21: 137–141.
8. Khan Z, Lafon M. PDZ domain-mediated protein interactions: therapeutic targets in neurological disorders. *Curr Med Chem* 2014, 21: 2632–2641.
9. Hillier BJ, Christopherson KS, Prehoda KE, Bredt DS, Lim WA. Unexpected modes of PDZ domain scaffolding revealed by structure of nNOS-syntrophin complex. *Science* 1999, 284: 812–815.
10. Wang Q, Hurd TW, Margolis B. Tight junction protein Par6 interacts with an evolutionarily conserved region in the amino terminus of PALS1/stardust. *J Biol Chem* 2004, 279: 30715–30721.
11. Liu W, Wen W, Wei Z, Yu J, Ye F, Liu CH, Hardie RC, *et al*. The INAD scaffold is a dynamic, redox-regulated modulator of signaling in the *Drosophila* eye. *Cell* 2011, 145: 1088–1101.
12. Ullmer C, Schmuck K, Figge A, Lubbert H. Cloning and characterization of MUPP1, a novel PDZ domain protein. *FEBS Lett* 1998, 424: 63–68.
13. Sitek B, Poschmann G, Schmidtke K, Ullmer C, Maskri L, Andriske M, Stichel CC, *et al*. Expression of MUPP1 protein in mouse brain. *Brain Res* 2003, 970: 178–187.
14. Estevez MA, Henderson JA, Ahn D, Zhu XR, Poschmann G, Lubbert H, Marx R, *et al*. The neuronal RhoA GEF, Tech, interacts with the synaptic multi-PDZ-domain-containing protein, MUPP1. *J Neurochem* 2008, 106: 1287–1297.
15. Jang WH, Choi SH, Jeong JY, Park JH, Kim SJ, Seog DH. Neuronal cell-surface protein neurexin 1 interaction with multi-PDZ domain protein MUPP1. *Biosci Biotechnol Biochem* 2014, 78: 644–646.
16. Shirley RL, Walter NA, Reilly MT, Fehr C, Buck KJ. Mpdz is a quantitative trait gene for drug withdrawal seizures. *Nat Neurosci* 2004, 7: 699–700.
17. Fehr C, Shirley RL, Metten P, Kosobud AE, Belknap JK, Crabbe JC, Buck KJ. Potential pleiotropic effects of Mpdz on vulnerability to seizures. *Genes Brain Behav* 2004, 3: 8–19.
18. Al-Dosari MS, Al-Owain M, Tulbah M, Kurdi W, Adly N, Al-Hemidan A, Masoodi TA, *et al*. Mutation in MPDZ causes severe congenital hydrocephalus. *J Med Genet* 2013, 50: 54–58.
19. Ali M, Hocking PM, McKibbin M, Finnegan S, Shires M, Poulter JA, Prescott K, *et al*. Mpdz null allele in an avian model of retinal degeneration and mutations in human leber congenital amaurosis and retinitis pigmentosa. *Invest Ophthalmol Vis Sci* 2011, 52: 7432–7440.
20. Milner LC, Shirley RL, Kozell LB, Walter NA, Kruse LC, Komiyama NH, Grant SG, *et al*. Novel MPDZ/MUPP1 transgenic and knockdown models confirm Mpdz's role in ethanol withdrawal and support its role in voluntary ethanol consumption. *Addict Biol* 2015, 20: 143–147.
21. Hamazaki Y, Itoh M, Sasaki H, Furuse M, Tsukita S. Multi-PDZ domain protein 1 (MUPP1) is concentrated at tight junctions through its possible interaction with claudin-1 and junctional adhesion molecule. *J Biol Chem* 2002, 277: 455–461.
22. Stiffler MA, Chen JR, Grantcharova VP, Lei Y, Fuchs D, Allen JE, Zaslavskaia LA, *et al*. PDZ domain binding selectivity is optimized across the mouse proteome. *Science* 2007, 317: 364–369.
23. Guillaume JL, Daulat AM, Maurice P, Levoye A, Migaud M, Brydon L, Malpaux B, *et al*. The PDZ protein mupp1 promotes Gi coupling and signaling of the Mt1 melatonin receptor. *J Biol Chem* 2008, 283: 16762–16771.
24. Barritt DS, Pearn MT, Zisch AH, Lee SS, Javier RT, Pasquale EB, Stallcup WB. The multi-PDZ domain protein MUPP1 is a cytoplasmic

ligand for the membrane-spanning proteoglycan NG2. *J Cell Biochem* 2000, 79: 213–224.
25. Yu C, Feng W, Wei Z, Miyanoiri Y, Wen W, Zhao Y, Zhang M. Myosin VI undergoes cargo-mediated dimerization. *Cell* 2009, 138: 537–548.
26. Wang H, Zhang Y, Zhang Z, Jin WL, Wu G. Purification, crystallization and preliminary X-ray analysis of the inverse F-BAR domain of the human srGAP2 protein. *Acta Crystallogr F Struct Biol Commun* 2014, 70: 123–126.
27. Krainer FW, Pletzenauer R, Rossetti L, Herwig C, Glieder A, Spadiut O. Purification and basic biochemical characterization of 19 recombinant plant peroxidase isoenzymes produced in Pichia pastoris. *Protein Expr Purif* 2014, 95: 104–112.
28. Skjoedt MO, Roversi P, Hummelshoj T, Palarasah Y, Rosbjerg A, Johnson S, Lea SM, *et al*. Crystal structure and functional characterization of the complement regulator mannose-binding lectin (MBL)/ficolin-associated protein-1 (MAP-1). *J Biol Chem* 2012, 287: 32913–32921.
29. Zhang DL, Wu LJ, Chen J, Liang Y. Effects of macromolecular crowding on the structural stability of human alpha-lactalbumin. *Acta Biochim Biophys Sin* 2012, 44: 703–711.
30. John DM, Weeks KM. van't Hoff enthalpies without baselines. *Protein Sci* 2000, 9: 1416–1419.
31. Pace CN, Scholtz JM. Measuring the conformational stability of a protein. In: Pace CN and Scholtz JM (eds). *Protein Structure: A Practical Approach*. 2nd edn. New York: Oxford University Press, 1997, 318–321.
32. Otwinowski Z, Minor W. Processing of X-ray diffraction data. *Methods Enzymol* 1997, 276: 307–326.
33. Murshudov GN, Skubak P, Lebedev AA, Pannu NS, Steiner RA, Nicholls RA, Winn MD, *et al*. REFMAC5 for the refinement of macromolecular crystal structures. *Acta Crystallogr D Biol Crystallogr* 2011, 67: 355–367.
34. Adams PD, Afonine PV, Bunkoczi G, Chen VB, Davis IW, Echols N, Headd JJ, *et al*. PHENIX: a comprehensive Python-based system for macromolecular structure solution. *Acta Crystallogr D Biol Crystallogr* 2010, 66: 213–221.
35. Emsley P, Lohkamp B, Scott WG, Cowtan K. Features and development of Coot. *Acta Crystallogr D Biol Crystallogr* 2010, 66: 486–501.
36. Larkin MA, Blackshields G, Brown NP, Chenna R, McGettigan PA, McWilliam H, Valentin F, *et al*. Clustal W and Clustal X version 2.0. *Bioinformatics* 2007, 23: 2947–2948.
37. Robert X, Gouet P. Deciphering key features in protein structures with the new ENDscript server. *Nucleic Acids Res* 2014, 42: W320–W324.
38. Leavitt S, Freire E. Direct measurement of protein binding energetics by isothermal titration calorimetry. *Curr Opin Struct Biol* 2001, 11: 560–566.
39. Kundu K, Backofen R. Cluster based prediction of PDZ–peptide interactions. *BMC Genomics* 2014, 15 Suppl 1: S5.
40. Songyang Z, Fanning AS, Fu C, Xu J, Marfatia SM, Chishti AH, Crompton A, *et al*. Recognition of unique carboxyl-terminal motifs by distinct PDZ domains. *Science* 1997, 275: 73–77.